Power Harmonics and Interharmonics Measurement Using Recursive Group-Harmonic Power Minimizing Algorithm

Hsiung Cheng Lin

***Abstract*—The discrete Fourier transform (DFT) is still a widely used tool for analyzing and measuring both stationary and transient signals in power system harmonics. However, the misapplications of the DFT can lead to incorrect results caused by some problems such as an aliasing effect, spectral leakage, and picket-fence effect. A strategy of recursive group-harmonic power minimizing algorithm is developed for systemwide harmonic/interharmonic evaluation in power systems. The proposed algorithm can restore the dispersing spectral leakage energy caused by the DFT and regain its harmonic/interharmonic magnitude and respective frequency. Every iteration loop for harmonic/interharmonic evaluation can guarantee to be convergent using the proposed group-harmonic bin power algorithm. Consequently, not only high precision in integer harmonic measurement can be retained but also the interharmonics can be accurately identified, particularly under system frequency drift. The numerical example is presented to verify the proposed algorithm in terms of robust, fast, and precise performance.**

***Index Terms*—Discrete Fourier transform (DFT), group harmonics, harmonics, interharmonics.**

I. Introduction

With increasing use of power electronic systems and time-variant nonlinear loads in industry, the generated power harmonics and interharmonics have resulted in serious power-line pollution. Power supply quality is therefore aggravated. Traditional harmonics may cause negative effects such as signal interference, overvoltage, data loss, equipment malfunction, equipment heating, and damage. The noise on data transmission line is also related with harmonics. At some special systems, harmonic current components may cause effect of carrier signals and thus interfere other carrier signals. As a result, some facilities may be affected. Once harmonics source enters computer instruments, the data stored in the computer may be lost up to ten times. Moreover, harmonics may also cause transformer and capacitor over heating, thus reducing their working life. The resulting rotor heating and pulsating output torque will decrease the driver's efficiency [1]–[8].

Manuscript received August 13, 2010; revised December 15, 2010 and March 1, 2011; accepted May 7, 2011. Date of publication May 19, 2011; date of current version October 18, 2011. This work was supported by the National Science Council of the Republic of China, Taiwan, under Grant NSC 99-2221-E-167-034.

The author is with the Department of Electronic Engineering, National Chin-Yi University of Technology, Taichung 411, Taiwan (e-mail: hclin@ncut.edu.tw).

Color versions of one or more of the figures in this paper are available online at http://ieeexplore.ieee.org.

Digital Object Identifier 10.1109/TIE.2011.2157281

The presence of power system interharmonics has not only brought many problems as harmonics but produced additional problems. For instance, there are thermal effects, low-frequency oscillation of mechanical system, light and cathode-ray-tube flicker, interference of control and protection signals, high-frequency overload of passive parallel filter, telecommunication interference, acoustic disturbance, saturation of current transformer, subsynchronous oscillations, voltage fluctuations, malfunctioning of remote control system, erroneous firing of thyristor apparatus, and the loss of useful life of induction motors. These phenomena may even happen under low amplitude [5], [9]–[12].

Conventionally, a discrete Fourier transform (DFT) method is efficient for signal spectrum evaluation because of the simplicity and easy implementation. An improper use of DFT-based algorithms can, however, lead to multiple interpretations of spectrum [12]–[14]. For example, if the periodicity of DFT data set does not match the periodicity of signal waveforms, the spectral leakage and picket-fence effect will occur. Since the power system frequency is subject to small random deviations, some degree of spectral leakage cannot be avoided. A number of algorithms, e.g., short-time Fourier transform [15], least square approach [16]–[18], Kalman filtering [19], [20], artificial neural networks [14], [21], have been proposed to extract harmonics. The approaches may either suffer from low solution accuracy or less computational efficiency. None is reported to perform well in interharmonic identification under system frequency variations although each demonstrates its specific advantages.

The presence of interharmonics strongly poses difficulties in modeling and measuring the distorted waveforms. This is mainly due to the following: 1) very low values of interests of interharmonics (about one order of quantity less than for harmonics); 2) the variability of their frequencies and amplitudes; 3) the variability of the waveform periodicity; and 4) the great sensitivity to the spectral leakage phenomenon. In recent years, the effect caused by interharmonics is apparently being worsened. Therefore, currently, the development of accurate interharmonics measurement has attracted great attention in both industry and academics. This point of view is fully supported by exploring a number of publications (2007–2010) related to this field [22]–[40]. However, the published outcome may still suffer from low accuracy, long computational time, complexity, or measurement limitation. Accordingly, it is still an essential research issue to be carried on in this field.

International Electrotechnical Commission (IEC) 61000-4-7 established a well-disciplined measurement method for harmonics/interharmonics. This standard has been recently revised to add methodology for measuring interharmonics [41]. The key to the measurement of both harmonics and interharmonics in the standard is the utilization of a 10- or 12-cycle sample window upon which to perform the Fourier transform. However, the spectrum resolution with 5 Hz is not sufficiently precise to reflect the practical interharmonic locations for both 50- and 60-Hz systems. This paper presents harmonic/interharmonic identification using a DFT-based RGPM approach, which retains the merits of a DFT analysis and extends to interharmonic identification under system frequency variation environments. This paper is organized as follows: Section II gives a background of the concept of system harmonic/interharmonic measurement. Section III presents the proposed RGPM algorithm. In Section IV, the model validation with a numerical example is demonstrated. Performance results under system frequency drift is included and discussed. Conclusion is given in Section V.

II. Background of System Harmonic/Interharmonic Measurement

A. Definition of Harmonic/Interharmonic

The integral multiple of alternating current (ac) system fundamental frequency is defined as harmonics of voltage or current signals. On the other hand, interharmonics is nonintegral multiple of ac system fundamental frequency, defined by IEC-1000-2-1 as follows [42].

"Between the harmonics of the power frequency voltage and current, further frequencies can be observed, which are not an integer of the fundamental. They can appear as discrete frequencies or as a wide-band spectrum."

The definition of harmonic/interharmonic is illustrated as follows.

1) Harmonic: $f_h = h \times f$, where h is an integer and greater than 0.
2) Direct current (dc): $f_h = 0$ Hz ($f_h = h \times f$, where $h = 0$).
3) Interharmonic: $f_i \neq h \times f$, where h is an integer and greater than 0.
4) Subharmonic: $f > f_h > 0$.

Note that f is the fundamental power system frequency, and subharmonic is a special case of interharmonic components.

B. Fundamental Concept of System Harmonics/Interharmonics

By Fourier theory, any repetitive distorted (nonsinusoidal) waveform $i_s(t)$ can be expressed as Fourier series of various sinusoidal frequencies (harmonics/interharmonics)

$$i_s(t) = \sum_{k=\infty}^{\infty} I_s(k\omega_0) e^{jk\omega_0 t} \tag{1}$$

$$I_s(k\omega_0) = \frac{1}{T} \int_{t}^{t+T} x(t) e^{-jk\omega_0 t} dt \tag{2}$$

where $\omega_0 (= 2\pi/T = 2\pi f)$ is the fundamental angular frequency, and $I_s(k\omega_0)$ is the kth coefficient.

Suppose the waveform $i_s(t)$ is sampled as N discrete points using sampling rate f_s. With the digital signal processing technology, the continuous signal $i_s(t)$ can be converted to a discrete signal $i_s[n]$ and then can be transformed by the DFT as

$$I_s[k] = \frac{1}{N} \sum_{n=0}^{N-1} i_s[n] W_N^{kn} \tag{3}$$

where $I_s[k]$ denotes the DFT of $i_s[n]$ at frequency f_k, i.e., $f_k = k/T$, and $W_N = \exp(j2\pi/N)$.

The inverse DFT, which allows us to recover the signal from its spectrum, is given by

$$i_s[n] = \sum_{k=0}^{N/2-1} I_s[k] W_N^{-kn}. \tag{4}$$

Assume that $i_s[n]$ is the periodic waveform with period T, and the angular frequency resolution $\Delta\omega$ is determined by the truncated signal length and defined as follows:

$$\Delta\omega = \frac{2\pi}{T}. \tag{5}$$

If the data sampling length is chosen as p ($p > 1$ and is an integer number) periods, $\Delta\omega$ can be rewritten as follows:

$$\Delta\omega = \frac{2\pi}{pT} = \frac{\omega_0}{p}. \tag{6}$$

According to (6), Δf can be expressed as

$$\Delta f = \frac{1}{pT} = \frac{1}{pN_sT_s} = \frac{1}{NT_s} = \frac{f_s}{N} \tag{7}$$

where $N_s \triangleq N/p$ and $T_s \triangleq 1/f_s$.

For instance, choose 10 60-Hz signal cycles for Fourier transform, and $\Delta f = 60/10 = 6$ Hz. Accordingly, 6, 12, 18 Hz, ... will appear in the spectrum, known as interharmonics. Furthermore, the executed time is $T_f = N \cdot 1/f_s$ if the signal is sampled N points by sampling rate f_s. Therefore, the Fourier fundamental period is expressed as T_f, i.e., $T_f = 1/\Delta f$.

C. Concept of Group Harmonic

The measurement of interharmonics is difficult with results depending on many factors. Based on the so-called "group" suggested by IEC 61000-4-7, the concept of group harmonic is introduced as follows [41].

By the Parseval relation in its discrete form, the power of waveform P can be expressed as [43], [44]

$$P = \frac{1}{N} \sum_{n=0}^{N/2-1} i_s[n]^2 = \sum_{k=0}^{N/2-1} I_s[k]^2. \tag{8}$$

Both positive and negative values of spectral components are considered to transform the frequency-dominant-sampled signal into a periodic time-dominant signal. Therefore, actual signals spectral components relevant to symmetrical frequencies are complex conjugates of each other. However, most

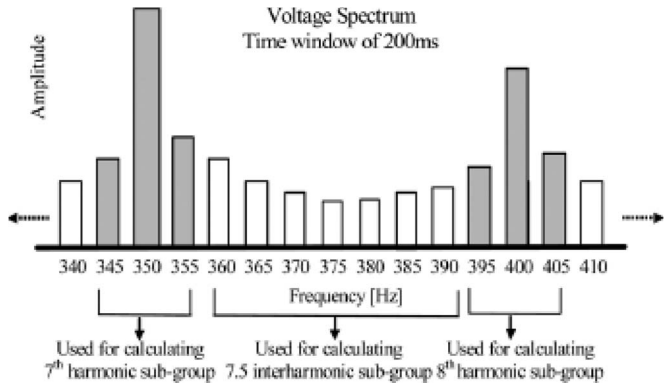

Fig. 1. IEC subgrouping of "bins" for both harmonics and interharmonics (graph reproduced from [5]).

real-world frequency analysis instruments display only the positive half of the frequency spectrum because the spectrum of a real-world signal is symmetrical around dc. Thus, the negative frequency information is redundant.

For this reason, the power at the discrete frequency f_k can be expressed as [44]

$$P[f_k] = I_s[k]^2 + I_s[N-k]^2 = 2I_s[k]^2 \tag{9}$$

where $k = 0, 1, 2, \ldots, N/2 - 1$.

The root-mean-square value of the harmonic amplitude at the discrete frequency f_k is

$$I_h[f_k] = \sqrt{P[f_k]} = \sqrt{2} I_s[k]. \tag{10}$$

The power of the harmonic at f_k may disperse over a frequency band around the f_k due to the spectral leakage. Hence, the total power of harmonics within the adjacent frequencies around f_k can be restored into a "group power" [13]. Each "group power," i.e., $P^*[f_k]$, can be collected between $f_{k-\Delta k}$ and $f_{k+\Delta k}$ as follows:

$$P^*[f_k] = \sum_{\Delta k=-\tau}^{+\tau} \left(I_h[f_{k+\Delta k}]\right)^2 \tag{11}$$

where τ is an integer number and denotes the group bandwidth.

Consequently, each harmonic amplitude can be estimated as

$$I_s^*[f_k] = \sqrt{P^*[f_k]}. \tag{12}$$

An interesting way to view this phenomenon is to observe the DFT implementation, shown in Fig. 1. Most leakages can be collected into one group and are considered as though they were all at the dominant harmonic frequency. The amplitude of interharmonics (and/or subharmonics) can be thus identified.

III. Proposed RGPM Algorithm

The power-line waveform $s(t)$ (voltage/current) is sampled using the sampling rate $f_s(= 1/T_s)$, which has the fundamental frequency f_d, as follows:

$$s(n) = s(t)\,|_{t=nT_s}\,, \quad n = 0, 1, 2, \ldots, N-1 \tag{13}$$

where N is the sampled point of Fourier fundamental period T_f.

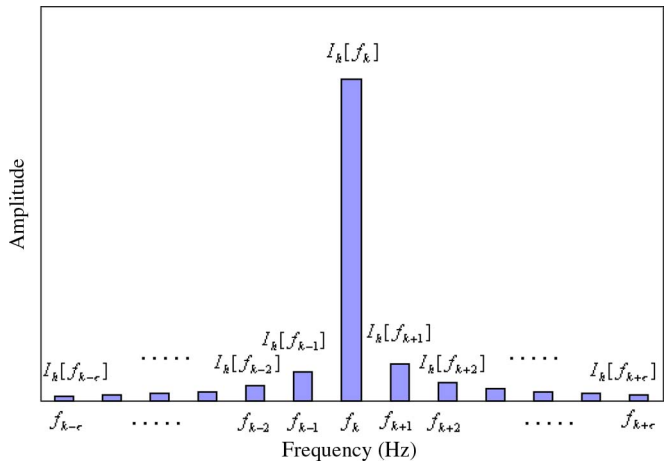

Fig. 2. Amplitude distribution around the dominant component.

In general, the distorted signal can be composed of three parts, as follows:

$$s(n) = s_d(n) + s_h(n) + s_i(n) \tag{14}$$

where $s_d(n)$ is the fundamental component, $s_h(n)$ is the harmonic components, and $s_i(n)$ represents the interharmonic components.

A. GBP Algorithm

Length N of the sampled window for the DFT analysis plays the critical point in determining if the spectrum can be accurately achieved. Based on the empirical observation using the DFT, Fig. 2 indicates that the second stronger amplitude is found to be located at the right side of the dominant component, i.e., $I_h[f_{k+1}] > I_h[f_{k-1}]$, in case of overlong truncated window. On the contrary, the second stronger amplitude is located at the left side of the dominant component, i.e., $I_h[f_{k+1}] < I_h[f_{k-1}]$, the truncated-window length is insufficient for the DFT analysis. Accordingly, the proposed RGPM approach is to develop the mechanism for correcting the window length according to the situation on the dispersed energy. This proposed RGPM method in deed extends the "group" concept that has been mentioned by IEC 61000-4-7 and some papers [5], [13], [44], [47].

The total dispersed power, i.e., $P^{**}[f_k]$, around the dominant frequency is defined as

$$P^{**}[f_k] = \sum_{\Delta k=-\tau}^{+\tau} \left(I_h[f_{k+\Delta k}]\right)^2 - \left(I_h[f_k]\right)^2 \tag{15}$$

where it denotes the dispersed bandwidth power, excluding the dominant component.

Based on the above concept, once the exact sampled window length N is found, $P^{**}[f_k]$ will reach the predefined minima power value $P_{\min}$. To guarantee the convergence of $P^{**}[f_k]$ with the procedure repetition, N should be therefore decreased if $I_h[f_{k+1}] > I_h[f_{k-1}]$, and N should be increased if $I_h[f_{k+1}] < I_h[f_{k-1}]$. The procedure will be repeated until

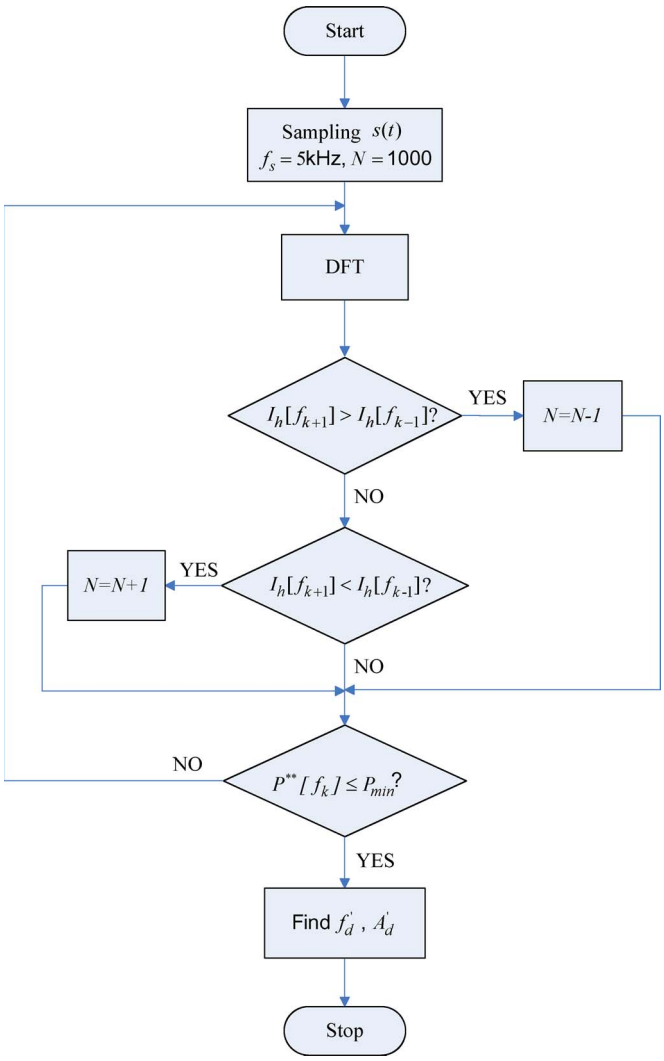

Fig. 3. Flowchart of the proposed GBP algorithm.

the minima power value is achieved; more details are shown in Fig. 3.

1) Set $f_s = 5$ kHz, and $N = 1000$ for sampling the power-line signal.
2) Implement the DFT.
3) If $I_h[f_{k+1}] > I_h[f_{k-1}]$, $N = N - 1$. Otherwise, go to the next step.
4) If $I_h[f_{k+1}] < I_h[f_{k-1}]$, $N = N + 1$. Otherwise, go to the next step.
5) Check if $P^{**}[f_k] \le P_{\min}$. If yes, the iteration loop stops, and determine the updated N. The fundamental frequency f_d' and amplitude A_d' can be thus obtained. Otherwise, go back to step 2 to repeat the procedure until $P^{**}[f_k] \le P_{\min}$.

B. Proposed RGPM Algorithm

In Fig. 4, the proposed recursive group-harmonic power minimizing (RGPM) algorithm that integrated with the group-harmonic bin power (GBP) algorithm is demonstrated as follows.

1) Determine the new $\Delta f' = f_s/N'$ using the GBP method, and find the correct fundamental frequency f_d' and its respective amplitude A_d'. Accordingly, the fundamental frequency signal $s_d'(n)$ and its harmonic signals $s_h'(n)$ can be obtained as follows:

$$s'(n) = s(t)\Big|_{t=\frac{n}{f_s'}} = s_d'(n) + s_h'(n) + s_i'(n), \quad n = 0, 1, 2, 3, \ldots, N' - 1 \quad (16)$$

2) Reconstruct the $s_d'(n)$ and $s_h'(n)$ and form a composed waveform. Therefore, the new waveform that only contains interharmonic components without $s_d'(n)$ and $s_h'(n)$ can be obtained as follows:

$$s_i'(n) = s'(n) - [s_d'(n) + s_h'(n)] \quad (17)$$

3) Assume the major interharmonic component (biggest amplitude) as the fundamental component.
4) Repeat steps 1)–3) until all major interharmonics are regained.

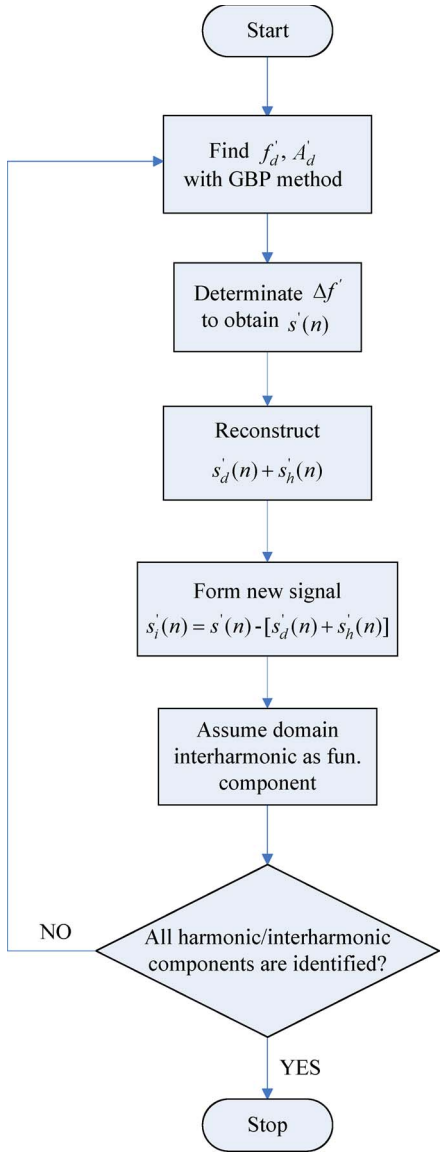

Fig. 4. Flowchart of the proposed RGPM algorithm.

IV. Model Validation With a Numerical Example

The proposed RGPM algorithm has been tested by the synthesized line signal (voltage/current) to verify the effectiveness of harmonic/interharmonic analysis. The following example is used to illustrate the harmonic analysis of a distorted waveform [45]–[47]:

$$\begin{aligned} s(t) = &\sin(2\pi f_d t + 23^\circ) + 0.25\sin(2\pi \cdot 3 \cdot f_d \cdot t + 68^\circ) \\ &+ 0.3\sin(2\pi \cdot 5 \cdot f_d \cdot t + 16^\circ) \\ &+ 0.3\sin(2\pi \cdot 128 \cdot t + 78^\circ) \\ &+ 0.15\sin(2\pi \cdot 243.2 \cdot t + 94^\circ) + 0.07\sin(2\pi \cdot 376 \cdot t) \end{aligned} \tag{18}$$

where $f_d = 60.32$ Hz is the fundamental frequency.

Generally, the system frequency drift is a concern in power systems because it may slightly vary from time to time due to the change of system loads. This effect, in deed, influences the traditional DFT spectrum analysis. As mentioned, the line signal has a fundamental frequency, i.e., 60.32 Hz, with 0.32-Hz drift and a scaled amplitude of 1 V. The third and fifth harmonic components are included in the synthesized waveform to present a possible distorted waveform situation. Noninteger components, i.e., interharmonic, such as 128, 243.2, and 376 Hz are to be considered, reflecting a possible polluted-line case. Note that the aforementioned harmonics/interharmonics are assigned different magnitudes and phases.

A. Selection of Group Bandwidth τ and Minima Power Value $P_{\min}$

The power of the harmonic at f_k may disperse over a frequency band around f_k due to spectral leakage, etc., when the DFT is used as a spectrum analysis tool. Therefore, each "group power" should be collected between $f_{k-\tau}$ and $f_{k+\tau}$ to ensure satisfactory spectrum results. Obviously, the larger group bandwidth τ can restore all leakages and regain the actual amplitude/frequency. However, with a large bandwidth, the "group power" may include considerable harmonic contents at distant frequencies because neighboring nominal harmonics may be widely dispersed. Additionally, the extracted frequency may be slightly apart from the actual value with a larger τ due to the influence of neighboring harmonic contents. As a consequence, group bandwidth τ should be chosen as large as possible for obtaining an accurate amplitude but small enough to avoid the overlap between two neighboring harmonic groups. Based on the results by this proposed RGPM model, group bandwidth τ is suggested to be chosen as $\tau = 4$ to reach the compromise.

On the other hand, minima power value $P_{\min}$ is a crucial factor to stop the iteration loop of the proposed GBP algorithm. Theoretically, $P_{\min}$ should be chosen as small as possible to achieve a more accurate result but relatively taking more iteration loops. Therefore, $P_{\min}$ is set as 0.001 with compromise in computational time, and the outcome is still satisfactory in this paper.

B. Spectrum Analysis

According to (17), we set $f_s = 5$ kHz, $N = 1000$, i.e., $\Delta f = 5$ Hz, and the waveform is shown in Fig. 5. As shown in Fig. 6, a considerable spectrum leakage occurs using the DFT so that the result is unable to represent its actual spectrum.

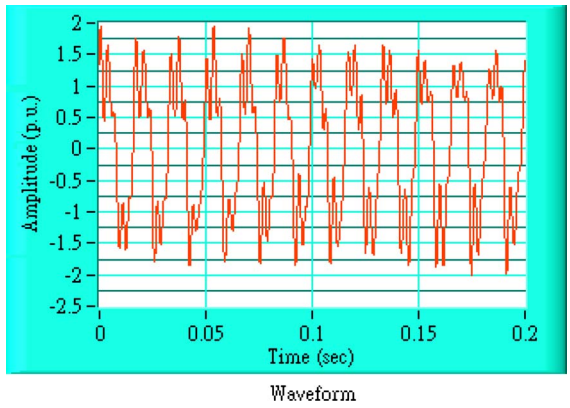

Fig. 5. Distorted waveform.

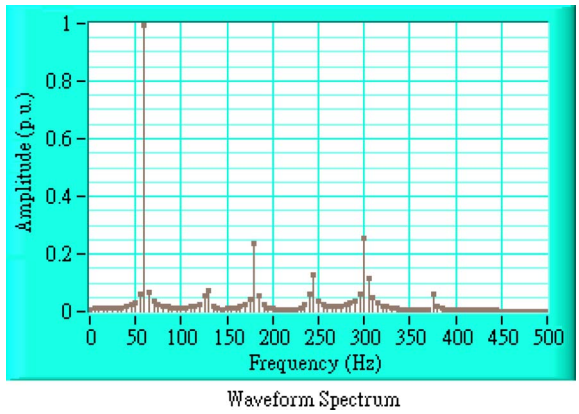

Fig. 6. Spectrum of the distorted waveform using the DFT.

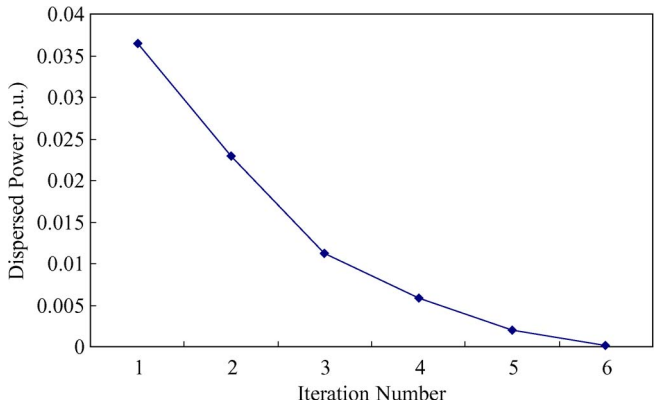

Fig. 7. Convergent curve of the dispersed power at the harmonic components.

Based on the proposed RGPM algorithm, the following steps are illustrated to find the true harmonics/interharmonics.

Step A—Measurement of Fundamental and Integer Harmonics With a 0.32-Hz Frequency Drift: In this case, the fundamental frequency component, including third and fifth harmonics, is considered to have a 0.32-Hz variation. The dispersed power of the harmonics over around the frequency band is significantly reduced from 0.0364 to 0.00011 within only six iteration loops, as shown in Fig. 7. Fig. 8 indicates that each harmonic is approaching toward its true amplitude

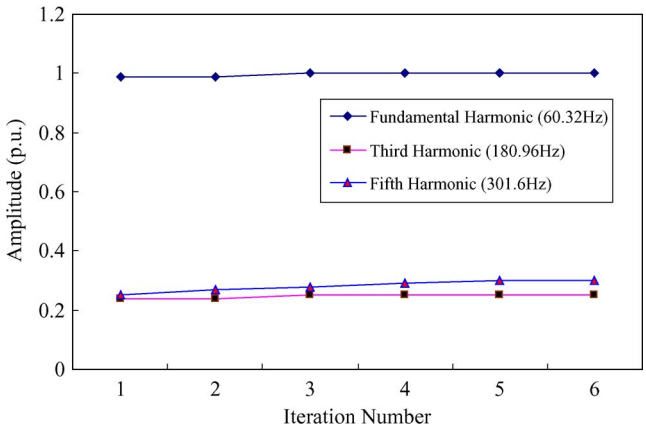

Fig. 8. Amplitude tracking curve of the harmonic components.

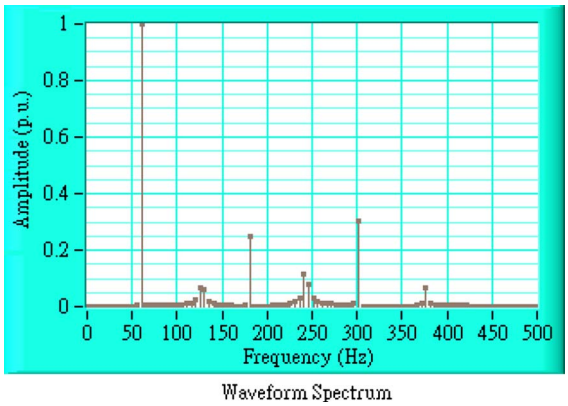

Fig. 9. Harmonic spectrum of the waveform using the RGPM algorithm.

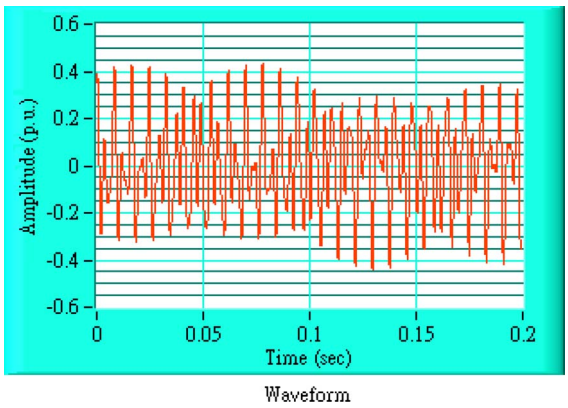

Fig. 10. Waveform with three interharmonics only.

step by step. The amplitudes of the fundamental, third, and fifth components are thus obtained as 1.0, 0.25, and 0.3 at the sixth iteration loop from 0.99, 0.24, and 0.25 at the first iteration loop, respectively. Additionally, the fundamental frequency is found as 60.32 Hz, matching the true one. Fig. 9 confirms that every harmonic spectrum, excluding interharmonics, has achieved its real value.

Step B—Measurement of the Interharmonic at 243.2 Hz: In this stage, all harmonic components acquired at Step A are excluded in the new waveform so that the interharmonic at 243.2 Hz is assumed as the fundamental component. The waveform and its spectrum using the DFT are shown in Figs. 10 and 11, respectively.

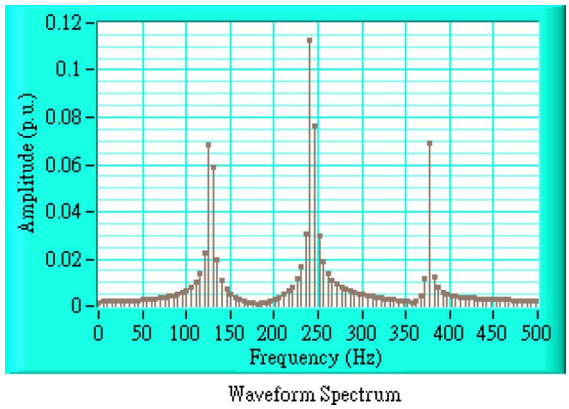

Fig. 11. Spectrum of the waveform using the DFT with three interharmonics only.

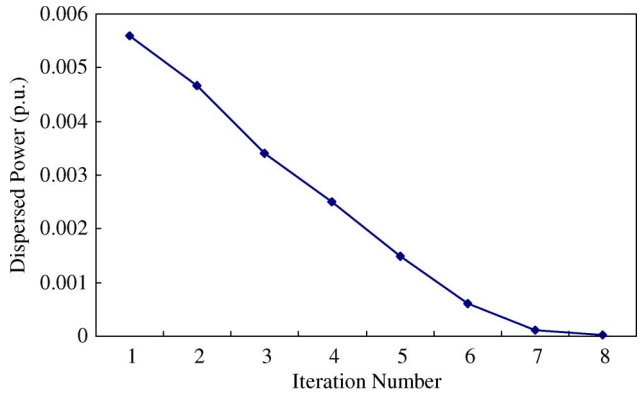

Fig. 12. Convergent curve of the dispersed power at the 243.2-Hz interharmonic.

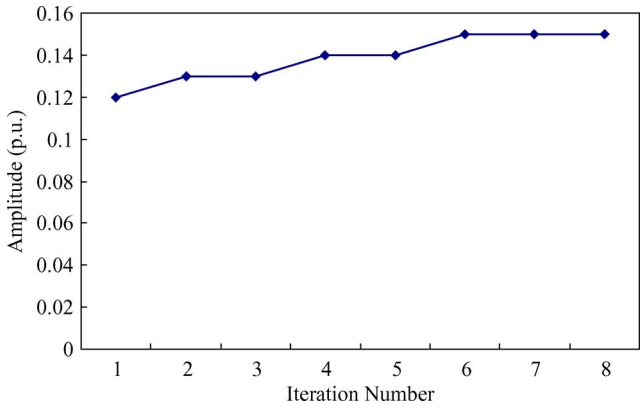

Fig. 13. Amplitude tracking curve of the 243.2-Hz interharmonic.

The dispersed power of the supposed fundamental band (interharmonic at 243.2 Hz) is considerably reduced from 0.0056 to 0.000012 within eight iteration loops, shown in Fig. 12. Accordingly, its amplitude is obtained as 0.15 from 0.12, and the 243.2-Hz component is thus confirmed, as shown in Figs. 13 and 14, respectively.

Step C—Measurement of the Interharmonic at 128 Hz: In this stage, all harmonics and 243.2-Hz interharmonic are excluded in the new waveform, as shown in Fig. 15. Therefore, only two interharmonics, i.e., 128 and 376 Hz, remained, and its spectrum using the DFT is shown in Fig. 16.

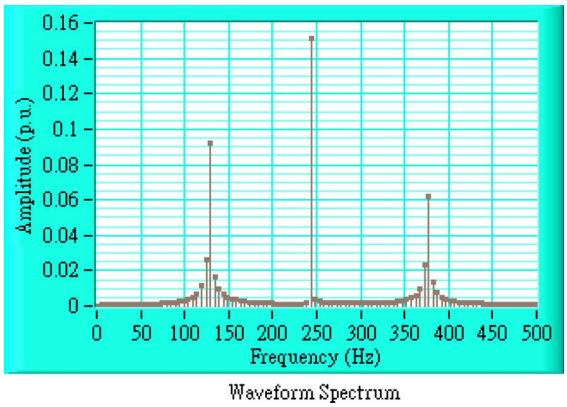

Fig. 14. Spectrum analysis using the RGPM algorithm at the 243.2-Hz interharmonic.

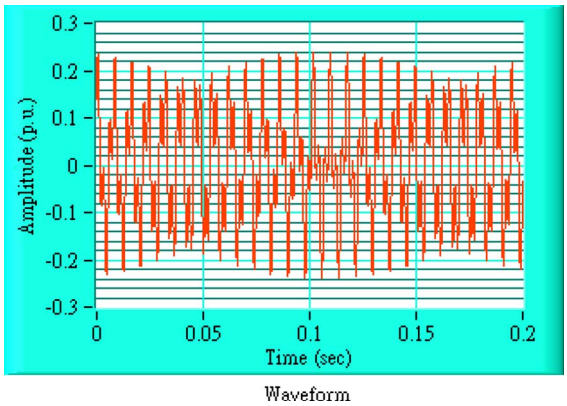

Fig. 15. Waveform with two interharmonics only.

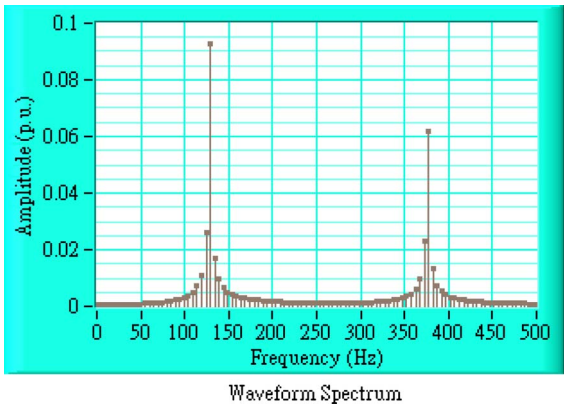

Fig. 16. Spectrum of the waveform using the DFT with two interharmonics only.

Similarly, the dispersed power of the supposed fundamental band (interharmonic at 128 Hz) is approaching toward to zero from 0.005 within 17 iteration loops, as shown in Fig. 17. Accordingly, its amplitude is obtained as 0.1 from 0.076, and the 128-Hz component is therefore confirmed, as shown in Figs. 18 and 19, respectively.

Step D—Measurement of the Interharmonic at 376 Hz: In the last stage, all harmonics, i.e., 243.2- and 128-Hz interharmonic, are excluded in the new waveform, as shown in Fig. 20. Therefore, only one interharmonic (376 Hz) remained, and its spectrum using the DFT is shown in Fig. 21.

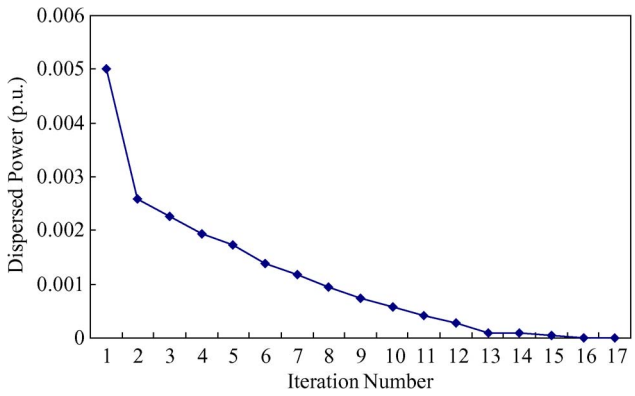

Fig. 17. Convergent curve of the dispersed power at the 128-Hz interharmonic.

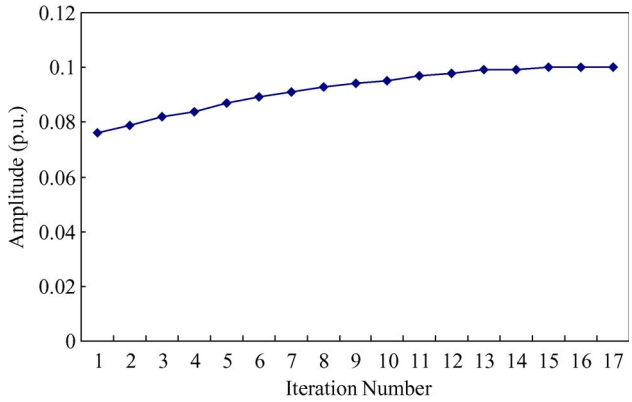

Fig. 18. Amplitude tracking curve of the 128-Hz interharmonic.

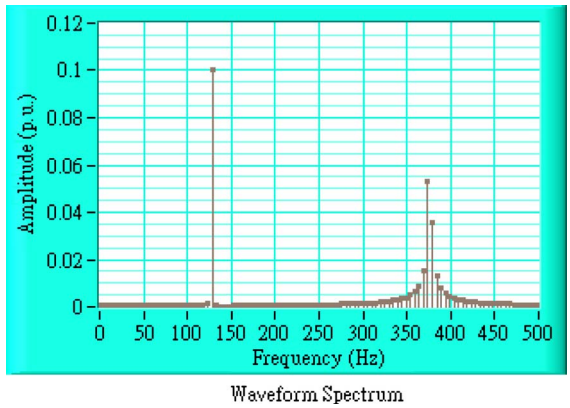

Fig. 19. Spectrum analysis using the RGPM algorithm at the 128-Hz interharmonic.

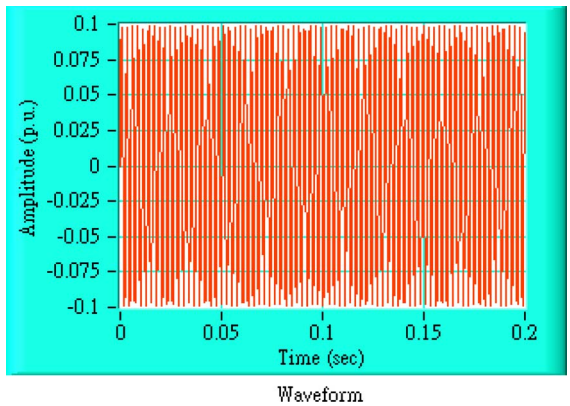

Fig. 20. Distorted waveform containing 376-Hz interharmonic only.

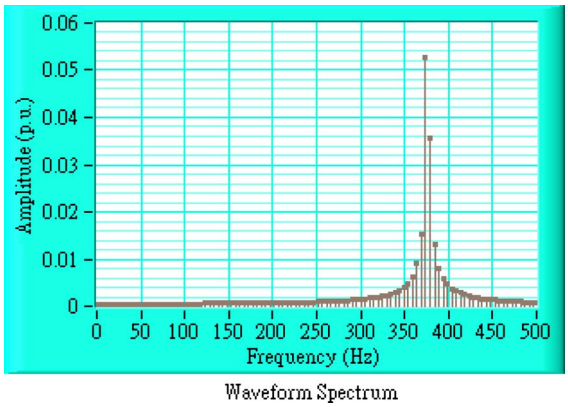

Fig. 21. Spectrum of the distorted waveform using the DFT for the 376-Hz interharmonic only.

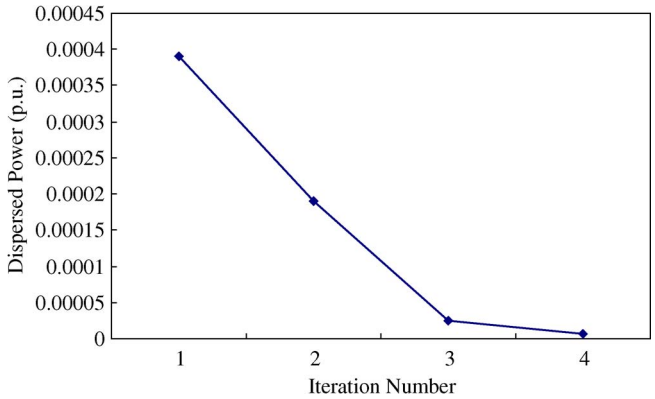

Fig. 22. Convergent curve of the dispersed power at the 376-Hz interharmonic.

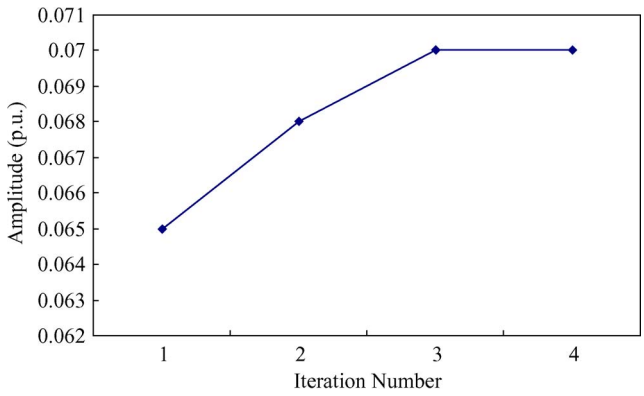

Fig. 23. Amplitude tracking curve of the 376-Hz interharmonic.

The dispersed power of the supposed fundamental band (interharmonic at 376 Hz) is quickly going down to almost zero from 0.00039 within only four iteration loops, as shown in Fig. 22. As a result, its amplitude is obtained as 0.07 from 0.065, and the 376-Hz component is thus confirmed, as shown in Figs. 23 and 24.

C. Comparison Between the DFT Analysis and the Proposed RGPM Model

The comparison between the DFT and the RGPM algorithm is listed in Tables I–VI, where τ is chosen as 4. Obviously, it is found that the dispersed amplitudes around the f_k, i.e.,

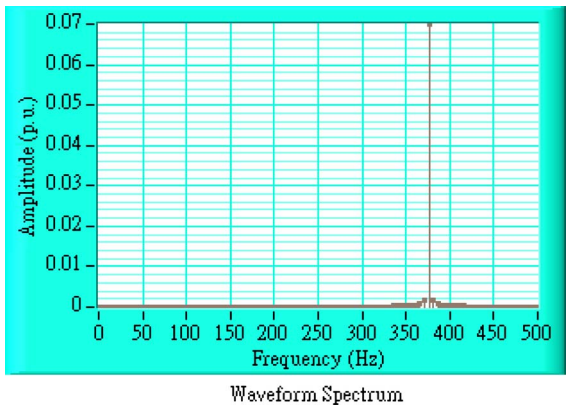

Fig. 24. Spectrum analysis using the RGPM algorithm at the 376-Hz interharmonic.

TABLE I
AMPLITUDE COMPARISON OF THE DFT AND THE RGPM AT $k = 12$ (FUNDAMENTAL HARMONIC)

k^{th}	f_{k-4}	f_{k-3}	f_{k-2}	f_{k-1}	f_k	f_{k+1}	f_{k+2}	f_{k+3}	f_{k+4}
Real	0	0	0	0	1	0	0	0	0
DFT	0.017	0.022	0.032	0.06	0.99	0.068	0.034	0.023	0.018
RGPM	0.003	0.003	0.003	0.004	1	0.006	0.005	0.004	0.004

TABLE II
AMPLITUDE COMPARISON OF THE DFT AND THE RGPM AT $k = 36$ (THIRD HARMONIC)

k^{th}	f_{k-4}	f_{k-3}	f_{k-2}	f_{k-1}	f_k	f_{k+1}	f_{k+2}	f_{k+3}	f_{k+4}
Real	0	0	0	0	0.25	0	0	0	0
DFT	0.013	0.016	0.023	0.04	0.24	0.053	0.022	0.013	0.009
RGPM	0.003	0.003	0.003	0.004	0.25	0.002	0.002	0.002	0.003

TABLE III
AMPLITUDE COMPARISON OF THE DFT AND THE RGPM AT $k = 60$ (FIFTH HARMONIC)

k^{th}	f_{k-4}	f_{k-3}	f_{k-2}	f_{k-1}	f_k	f_{k+1}	f_{k+2}	f_{k+3}	f_{k+4}
Real	0	0	0	0	0.3	0	0	0	0
DFT	0.023	0.028	0.038	0.064	0.25	0.12	0.046	0.028	0.02
RGPM	0.008	0.008	0.008	0.01	0.3	0.002	0.001	0.002	0.002

TABLE IV
AMPLITUDE COMPARISON OF THE DFT AND THE RGPM AT $k = 49$ (243.2-HZ INTERHARMONIC)

k^{th}	f_{k-4}	f_{k-3}	f_{k-2}	f_{k-1}	f_k	f_{k+1}	f_{k+2}	f_{k+3}	f_{k+4}
Real	0	0	0	0	0.15	0	0	0	0
DFT	0.009	0.014	0.024	0.065	0.12	0.034	0.021	0.015	0.012
RGPM	0.0009	0.0007	0.0008	0.002	0.15	0.004	0.003	0.002	0.002

TABLE V
AMPLITUDE COMPARISON OF THE DFT AND THE RGPM AT $k = 26$ (128-HZ INTERHARMONIC)

k^{th}	f_{k-4}	f_{k-3}	f_{k-2}	f_{k-1}	f_k	f_{k+1}	f_{k+2}	f_{k+3}	f_{k+4}
Real	0	0	0	0	0.1	0	0	0	0
DFT	0.008	0.011	0.018	0.05	0.076	0.022	0.013	0.010	0.008
RGPM	0.0008	0.001	0.002	0.004	0.1	0.004	0.002	0.002	0.001

TABLE VI
AMPLITUDE COMPARISON OF THE DFT AND THE RGPM AT $k = 75$ (376-HZ INTERHARMONIC)

k^{th}	f_{k-4}	f_{k-3}	f_{k-2}	f_{k-1}	f_k	f_{k+1}	f_{k+2}	f_{k+3}	f_{k+4}
Real	0	0	0	0	0.07	0	0	0	0
DFT	0.0031	0.004	0.0059	0.011	0.065	0.016	0.0073	0.0047	0.0047
RGPM	0.0004	0.0006	0.0009	0.0018	0.07	0.002	0.0009	0.0006	0.0004

$f_{k-4} - f_{k-1}$ and $f_{k+1} - f_{k+4}$, are too apparent to be ignored by the DFT. On the other hand, the proposed RGPM model can effectively reduce all dispersed power to almost zero and thus guarantee true amplitudes/frequency to be achieved. Tables I–III indicate that the amplitudes of the fundamental, third, and fifth harmonics at f_k by the DFT are calculated as 0.99, 0.24, and 0.25, respectively. With the proposed RGPM method, their actual amplitudes can be accurately obtained as 1.0, 0.25, and 0.3. In Table IV, the amplitude of the 243.2-Hz interharmonic using the DFT at f_k is computed as 0.12, and the RGPM can achieve its actual value, i.e., 0.15. Similarly, Tables V and VI reveal that small distortion caused by 128- and 376-Hz interharmonics at f_k can be accurately evaluated as 0.1 and 0.07, respectively, by the RGPM.

D. Discussion About Stability and Measuring Time Length of Respective Signal

As we know, it cannot avoid spectral leakage caused by uncertainty between frequency resolution and measuring time length using the DFT. As a result, normally, an appropriate window, such as Hamming and Blackman windows, is used to reduce spectral leakage with compromise in frequency resolution. However, it is not applicable in the presence of interharmonics due to some difficulties, e.g., variability in their frequencies and amplitudes or waveform periodicity.

In practice, the change of respective signal may result in its spectrum somewhat broad. As shown, a considerable spectrum leakage always occurs using the DFT so that its spectrum cannot represent an actual one. This phenomenon has been fully studied with the proposed RGPM approach that can retrieve all dispersed bandwidth power, even when the target line spectra may be nonstationary in their frequencies and amplitudes. Every interharmonic component that is initially assumed as the fundamental component can be identified using the mechanism of the proposed GBP algorithm but requiring some iterations only. For example, in Section IV-B, the measurement of fundamental and integer harmonics with a 0.32-Hz frequency drift requires six iteration loops. The measurement of the interharmonic at 128 Hz needs 17 iteration loops. In addition, the interharmonics at 243.2 and 376 Hz require eight and four iteration loops, respectively, to be recognized.

Obviously, the simulation results confirm that the proposed scheme is capable of performing a fast computation for extracting accurate interharmonics because it requires only tens of iteration loops and thus achieves a satisfactory outcome. Furthermore, the measuring time length of respective signal is based on the DFT so that only one signal acquisition is demanded to implement the proposed scheme.

E. Discussion About Industrial Application

The proposed RGPM algorithm is an advanced DFT-based method for an interharmonic analysis. Accordingly, for the practical application of the methodology in industry, the RGPM algorithm can be easily added to such DFT-based measurement devices that are still currently widely used. Alternatively, the RGPM algorithm is suitable for online microprocessed implementation if the DFT is available with input/output interface capability in the chip.

The interharmonic amplitude and frequency, even phase under different system frequency drifts, may vary in the power system any time. The RGPM algorithm is quickly adaptive to any variation of system frequency in power systems. Consequently, most measurement devices that have some inherent errors caused by interharmonic leakages can be fixed by using the RGPM algorithm, and the robustness of the algorithm can be thus guaranteed.

V. Conclusion

Although the DFT has certain limitations in the harmonic analysis, it is still widely used in the industry today. The harmonic/interharmonic identification using a DFT-based RGPM algorithm has been developed to be accurately and efficiently extracted. The test results confirm that the proposed RGPM method can guarantee the tracking of each harmonic/interharmonic amplitude to be convergent at every iteration loop by the GBP algorithm. There is no theoretical restriction in the locations of the interharmonic components while group bandwidth τ of each harmonic/interharmonic should be appropriately chosen. Moreover, the RGPM methodology has been successfully implemented by a Laboratory Virtual Instrumentation Engineering Workbench programming so that it can be easily extended to other software packages such as a microprocessor for online measurement. Additionally, the proposed RGPM can provide an advanced improvement for most measurement devices with some inherent errors because of the spectrum leakages caused by harmonics/interharmonics.

References

[1] M. B. Rifai, T. H. Ortmeyer, and W. J. McQuillan, "Evaluation of current interharmonics from AC drives," *IEEE Trans. Power Del.*, vol. 15, no. 3, pp. 1094–1098, Jul. 2000.

[2] H. Qian, R. Zhao, and T. Chen, "Interharmonics analysis based on interpolating windowed FFT algorithm," *IEEE Trans. Power Del.*, vol. 22, no. 2, pp. 1064–1069, Apr. 2007.

[3] Q. Zhang, H. Liu, H. Chen, Q. Li, and Z. Zhang, "A precise and adaptive algorithm for interharmonics measurement based on iterative DFT," *IEEE Trans. Power Del.*, vol. 23, no. 4, pp. 1728–1735, Oct. 2008.

[4] G. W. Chang, C. Y. Chen, and M. C. Wu, "A modified algorithm for harmonics and interharmonics measurement," in *Proc. IEEE Power Eng. Soc. Gen. Meeting*, Jun. 24–28, 2007, pp. 1–5.

[5] A. Testa, M. F. Akram, R. Burch, G. Carpinelli, G. Chang, V. Dinavahi, C. Hatziadoniu, W. M. Grady, E. Gunther, M. Halpin, P. Lehn, Y. Liu, R. Langella, M. Lowenstein, A. Medina, T. Ortmeyer, S. Ranade, P. Ribeiro, N. Watson, J. Wikston, and W. Xu, "Interharmonics: Theory and modeling," *IEEE Trans. Power Del.*, vol. 22, no. 4, pp. 2335–2348, Oct. 2007.

[6] D. E. Steeper and R. P. Stratford, "Reactive compensation and harmonic suppression for industrial power systems using thyristor converters," *IEEE Trans. Ind. Appl.*, vol. IA-12, no. 3, pp. 232–254, May 1976.

[7] K. H. Sueker, S. D. Hummel, and R. D. Argent, "Power factor correction and harmonic mitigation in a thyristor controlled glass melter," *IEEE Trans. Ind. Appl.*, vol. 25, no. 6, pp. 972–975, Nov./Dec. 1989.

[8] H. C. Lin, "Fast tracking of time-varying power system frequency and harmonics using iterative-loop approaching algorithm," *IEEE Trans. Ind. Electron.*, vol. 54, no. 2, pp. 974–983, Apr. 2007.

[9] D. Gallo, R. Langella, and A. Testa, "Interharmonics, Part 1: Aspects related to modeling and simulation," in *Proc. 6th Int. Workshop Power Definitions Meas. Under Non-Sinusoidal Conditions*, Milano, Italy, Oct. 13–15, 2003, pp. 168–173.

[10] D. Gallo, R. Langella, and A. Testa, "Interharmonics, Part 2: Aspects related to measurement and limits," in *Proc. 6th Int. Workshop Power Definitions Meas. Under Non-Sinusoidal Conditions*, Milano, Italy, Oct. 13–15, 2003, pp. 174–181.

[11] J. Barros, E. Prez, A. Pigazo, and R. I. Diego, "Simultaneous measurement of harmonics, interharmonics and flicker in a power system for power quality analysis," in *Proc. 5th Int. Conf. Power Syst. Manag. Control*, Apr. 17–19, 2002, pp. 100–105.
[12] M. Karimi-Ghartemani and M. R. Iravani, "Measurement of harmonics/inter-harmonics of time-varying frequency," *IEEE Trans. Power Del.*, vol. 20, no. 1, pp. 23–31, Jan. 2005.
[13] C. S. Moo and Y. N. Chang, "Group-harmonic identification in power systems with nonstationary waveforms," in *Proc. Inst. Elect. Eng.—Gener. Transm. Distrib.*, Sep. 1995, vol. 142, no. 5, pp. 517–522.
[14] H. C. Lin, "Intelligent neural network based adaptive power line conditioner for real-time harmonics filtering," *Proc. Inst. Elect. Eng.—Gener. Transm. Distrib.*, vol. 151, no. 5, pp. 561–567, Sep. 2004.
[15] H. K. Kwok and D. L. Jones, "Improved instantaneous frequency estimation using an adaptive short-time Fourier transform," *IEEE Trans. Signal Process.*, vol. 48, no. 10, pp. 2964–2972, Oct. 2000.
[16] S. A. Soliman, R. A. Alammari, M. E. El-Hawary, and M. A. Mostafa, "Effects of harmonic distortion on the active and reactive power measurements in the time dominant: A single phase system," in *Proc. IEEE Power Tech.*, Sep. 10–13, 2001, vol. 1, p. 6.
[17] M. Bettayeb and U. Qidwai, "Recursive estimation of power system harmonics," *Elect. Power Syst. Res.*, vol. 47, no. 2, pp. 143–152, Oct. 1998.
[18] A. Al-Kandari and K. M. El-Naggar, "Time dominant modeling and identification of nonlinear loads using discrete time-filtering estimator," in *Proc. IEEE Transm. Distrib. Conf. Expo.*, Sep. 7–12, 2003, vol. 1, pp. 126–131.
[19] A. A. Girgis, W. B. Chang, and E. B. Makram, "A digital recursive measurement scheme for on-line tracking of power system harmonics," *IEEE Trans. Power Del.*, vol. 6, no. 3, pp. 1153–1160, Jul. 1991.
[20] J. A. Macias and A. Gomez, "Self-tuning of Kalman filters for harmonic computation," *IEEE Trans. Power Del.*, vol. 21, no. 1, pp. 501–503, Jan. 2006.
[21] H. C. Lin, "Intelligent neural network based fast power system harmonic detection," *IEEE Trans. Ind. Electron.*, vol. 54, no. 1, pp. 43–52, Feb. 2007.
[22] J. Yong, T. Tayjasanant, X. Wilsun, and C. Sun, "Characterizing voltage fluctuations caused by a pair of interharmonics," *IEEE Trans. Power Del.*, vol. 23, no. 1, pp. 319–327, Jan. 2008.
[23] A. Miron, M. Chindris, and A. Cziker, "Interharmonics analysis using Fourier transform and virtual instrumentation," in *Proc. 10th Int. Conf. EPQU*, Sep. 15–17, 2009, pp. 1–4.
[24] T. Kim, E. J. Powers, W. M. Grady, and A. Arapostathis, "Detection of flicker caused by interharmonics," *IEEE Trans. Instrum. Meas.*, vol. 58, no. 1, pp. 152–160, Jan. 2009.
[25] G. Wiczynski, "Standard measurement of interharmonics in a power supply system while evaluating obnoxiousness of a flicker," in *Proc. 13th ICHQP*, Sep. 28–Oct. 1 2008, pp. 1–4.
[26] B. E. Kushare, A. A. Ghatol, and M. S. Aphale, "Survey of interharmonics in Indian power system network," in *Proc. IPEC*, Dec. 3–6, 2007, pp. 1230–1235.
[27] G. W. Chang, C.-I. Chen, and Q.-W. Liang, "A two-stage ADALINE for harmonics and interharmonics measurement," *IEEE Trans. Ind. Electron.*, vol. 56, no. 6, pp. 2220–2228, Jun. 2009.
[28] J. Valenzuela and J. Pontt, "Real-time interharmonics detection and measurement based on FFT algorithm," in *Proc. AE*, Sep. 9–10, 2009, pp. 259–264.
[29] T. Kim, A. Wang, E. J. Powers, W. M. Grady, and A. Arapostathis, "Detection of flicker caused by high-frequency interharmonics," in *Proc. IEEE Instrumen. Meas. Technol. Conf.*, May 1–3, 2007, pp. 1–5.
[30] T. X. Zhu, "Exact harmonics/interharmonics calculation using adaptive window width," *IEEE Trans. Power Del.*, vol. 22, no. 4, pp. 2279–2288, Oct. 2007.
[31] P. B. Petrovic and M. R. Stevanovic, "Digital processing of synchronously sampled AC signals in the presence of interharmonics and subharmonics," *IEEE Trans. Instrum. Meas.*, vol. 56, no. 6, pp. 2584–2598, Dec. 2007.
[32] J. Drapela, "A time domain based flickermeter with response to high frequency interharmonics," in *Proc. 13th ICHQP*, Sep. 28–Oct. 1, 2008, pp. 1–7.
[33] G. W. Chang, C. I. Chen, Y. J. Liu, and M. C. Wu, "Measuring power system harmonics and interharmonics by an improved fast Fourier transform-based algorithm," *IET Gener. Transm. Distrib.*, vol. 2, no. 2, pp. 193–201, Mar. 2008.
[34] J. San Martin, J. Pontt, F. Bello, and R. Aguilera, "Interharmonics power losses estimation in power transformer fed high power cycloconverter drive," in *Conf. Rec. IEEE IAS Annu. Meeting*, Oct. 5–9, 2008, pp. 1–5.
[35] S. M. Halpin and V. Singhvi, "Limits for interharmonics in the 1–100-Hz range based on lamp flicker considerations," *IEEE Trans. Power Del.*, vol. 22, no. 1, pp. 270–276, Jan. 2007.
[36] I. Y.-H. Gu and M. H. J. Bollen, "Estimating interharmonics by using sliding-window ESPRIT," *IEEE Trans. Power Del.*, vol. 23, no. 1, pp. 13–23, Jan. 2008.
[37] P. B. Petrovic, "Calculation of measurements uncertainties in case of asynchronous sampling of complex AC signals," in *Proc. IEEE IMTC*, May 12–15, 2008, pp. 1701–1706.
[38] K. S. Smith and L. Ran, "Torsional resonance risk management in islanded industrial power systems supplying large VFDs," *IEEE Trans. Ind. Appl.*, vol. 44, no. 6, pp. 1841–1850, Nov./Dec. 2008.
[39] P. Wei, J. Li, and Z. Li, "Interharmonics monitoring of power network using modified covariance arithmetic and virtual instrument," in *Proc. 9th ICEMI*, Aug. 16–19, 2009, pp. 3-242–3-245.
[40] C.-I. Chen and G. W. Chang, "Virtual instrumentation and educational platform for time-varying harmonic and interharmonic detection," *IEEE Trans. Ind. Electron.*, vol. 57, no. 10, pp. 3334–3342, Oct. 2010.
[41] Testing and Measurement Techniques: Harmonics and Interharmonics: General Guide on Harmonics and Interharmonics Measurements and Instrumentation for Power Supply Systems and Equipment Connected Thereto, IEC 61 000-4-7, 2002.
[42] *Electromagnetic Compatibility, Part 2: Environment, Sect. 1: Description of the Environment-Electromagnetic Environment for Low-Frequency Conducted Disturbances and Signalling in Public Power Supply Systems*, CEI/IEC 1000-2-1:1990, 1990-05.
[43] A. V. Oppenheim and R. W. Schafer, *Discrete-Time Signal Processing*. Englewood Cliffs, NJ: Prentice-Hall, 1989.
[44] W. H. Press, B. P. Flannery, S. A. Teukolsky, and W. T. Vetterling, *Numerical Recipes—The Art of Scientific Computing*. Cambridge, U.K.: Cambridge Univ. Press, 1986, pp. 420–429.
[45] H. C. Lin and C. S. Lee, "Enhanced FFT based parametric algorithm for simultaneous multiple harmonics analysis," in *Proc. Inst. Elect. Eng.—Gener. Transm. Distrib.*, May 2001, vol. 148, no. 3, pp. 209–214.
[46] T. T. Nguyen, "Parametric harmonic analysis," *Proc. Inst. Elect. Eng.—Gener. Transm. Distrib.*, vol. 144, no. 1, pp. 21–25, Jan. 1997.
[47] V. L. Pham and K. P. Wong, "Wavelet-transform-based algorithm for harmonic analysis of power system waveforms," *Proc. Inst. Elect. Eng.—Gener. Transm. Distrib.*, vol. 146, no. 3, pp. 249–254, May 1999.

Hsiung Cheng Lin was born in Changhua, Taiwan, on September 3, 1962. He received the B.S. degree from National Taiwan Normal University, Taipei, Taiwan, in 1986, and the M.S. and Ph.D. degrees from Swinburne University of Technology, Melbourne, Australia, in 1995 and 2002, respectively.

He was a Lecturer and an Associate Professor with Chung Chou Institute of Technology, Yuanlin, Taiwan. He was a Professor with the Department of Automation Engineering, Chienkuo Technology University (CTU), Changhua. He is currently a Professor with the Department of Electronic Engineering, National Chin-Yi University of Technology, Taichung, Taiwan. His special fields of interest include power electronics, neural network, network supervisory system, and adaptive filter design.

Dr. Lin was the recipient of the excellent teaching award from CTU in 2005, 2006, and 2007. He was also nominated and included in the first edition of *Who's Who in Asia* in 2007 and the tenth edition of *Who's Who in Science and Engineering* in 2007.